Fuel Processing Technology 234 (2022) 107333

Contents lists available at ScienceDirect

Fuel Processing Technology

journal homepage: www.elsevier.com/locate/fuproc

Enhanced hydrogen production using a tandem biomass pyrolysis and plasma reforming process

Weitao Wang [a], Yan Ma [b], Guoxing Chen [c,*], Cui Quan [b], Jale Yanik [d], Ningbo Gao [b,*], Xin Tu [a,*]

[a] Department of Electrical Engineering and Electronics, University of Liverpool, Liverpool L69 3GJ, United Kingdom
[b] Xi'an International Joint Research Center for Solid Waste Recycling and Utilization, School of Energy and Power Engineering, Xi'an Jiaotong University, Xi'an, 710049, China
[c] Fraunhofer Research Institution for Materials Recycling and Resource Strategies IWKS, Brentanostraße 2a, 63755 Alzenau, Germany
[d] Department of Chemistry, Faculty of Science, Ege University, 35100 Bornova, Izmir, Turkey

ARTICLE INFO

Keywords:
Biomass pyrolysis
Cellulose
Reforming
Non-thermal plasmas
Plasma catalysis
H_2 production

ABSTRACT

Converting biomass into energy and fuels is considered a promising strategy for replacing the exhaustible fossil fuels. In this study, we report on a tandem process that combines cellulose pyrolysis and plasma-assisted reforming for H_2 production. The hybrid pyrolysis/plasma reforming process was carried out in a two-stage reaction system incorporating a coaxial dielectric barrier discharge (DBD) plasma reactor. The effects of discharge power, steam, reforming temperature, and catalyst on the reaction performance were investigated. The results show that low temperatures are preferred in the non-catalytic plasma reforming process, whereas high temperatures are desired to achieve a high H_2 yield and a high H_2 selectivity in the plasma-catalytic reforming system. The synergistic effect of plasma catalysis was dominant in the plasma-catalytic reforming process at 250 °C. In contrast, the catalyst, rather than the plasma, played a dominant role in the plasma-catalytic reforming at higher temperatures (550 °C). Using Ni-Co/Al_2O_3 at a reforming temperature of 550 °C, a high H_2 yield of 26.6 mmol/g was attainted, which was more than 8 times and about 100% greater than that obtained using plasma alone and catalyst alone, respectively. This work highlights the potential of non-thermal plasmas in low-temperature biomass conversion.

1. Introduction

There is an increasing demand for sustainable energy production that relies on renewable energy sources and feedstocks to replace exhaustible fossil fuels. Biomass is a promising renewable energy source because of its abundance and the benefit of eliminating carbon dioxide from the atmosphere through biomass growth [1–3]. It can be obtained from a variety range of sources (e.g., wood, wood waste, agricultural crops, municipal wastes, and animal wastes) [4]. In addition, biomass-based fuels as an alternative to fossil fuels could help to mitigate severe environmental issues such as global warming [5–7]. According to the Office for National Statistics of the United Kingdom [8], biomass has become the largest renewable energy source in the UK, accounting for around 40% of renewable energy consumption and contributing to the UK's ambition to achieve net-zero carbon emissions by 2050. Biomass can be burned directly for heat and electricity or transformed into valuable liquid and gaseous fuels via a variety of processes including thermochemical [2], biological [9], and electrochemical processes [10]. However, direct combustion of biomass as an energy source, on the other hand, produces pollutants like NO_x and SO_x, as well as greenhouse gases like CO_2, exacerbating the environmental problems [11]. In comparison, the route (e.g., pyrolysis/gasification) to convert biomass into fuels is particularly appealing because it has the potential to produce valuable products such as hydrogen. Hydrogen has nearly three times the energy capacity of gasoline and is regarded as the best alternative source of energy as it only produces H_2O as a byproduct of combustion [12]. Furthermore, H_2 is a critical feedstock in petroleum refining [13], as well as the production of ammonia [14,15], methanol [16], ethanol [17] and other chemicals [18].

Numerous studies on the pyrolysis/gasification of various biomass (e.g., lignin, cellulose, and hemicellulose) have been conducted to date [19–21]. However, contamination of products with tar is one of the major challenges in thermochemical conversion of biomass (e.g., pyrolysis/gasification). As a result, significant efforts have been made to

* Corresponding authors.
E-mail addresses: guoxing.chen@iwks.fraunhofer.de (G. Chen), nbogao@xjtu.edu.cn (N. Gao), xin.tu@liverpool.ac.uk (X. Tu).

https://doi.org/10.1016/j.fuproc.2022.107333
Received 5 April 2022; Received in revised form 15 May 2022; Accepted 19 May 2022
Available online 1 June 2022

integrate thermochemical (e.g., pyrolysis/gasification) conversion of biomass with subsequent high temperature catalytic reforming for clean hydrogen generation [22–24]. Previous works [23–26], for example, reported the use of nickel-based catalysts in the pyrolysis/reforming of biomass for enhanced hydrogen production with a low tar formation. However, high temperatures are always required in these processes, particularly in the reforming process, which consumes a significant amount of energy. Wu et al. [23] employed a two-stage reaction system for hydrogen production from pyrolysis/reforming of various biomass feedstocks, with the temperature of the reforming process in the second stage fixed at 800 °C, 300 °C higher than that used in the first stage pyrolysis process. Furthermore, rapid catalyst deactivation caused by coke deposition remains a significant challenge in the catalytic biomass reforming process [27].

Non-thermal plasma (NTP) technology has recently attracted intense interest of researchers in the reforming of tar, a common undesirable product produced during biomass pyrolysis/gasification to produce syngas or hydrogen [28–35]. NTP technology has the advantage of being able to operate at lower temperatures than traditional catalytic processes [36–38]. NTPs generate highly energetic electrons with a typical electron energies ranging from 1 to 10 eV [39], while the plasma gas temperature can remain as low as room temperature. The energetic electrons in the plasma can easily break chemical bonds, resulting in an avalanche of reactive species (e.g., ions, free radicals, and excited atoms and molecules), allowing thermodynamically unfavorable reactions to occur at atmospheric pressure and low temperatures. However, NTP-based reforming processes are generally associate with low syngas yield and selectivity [40]. This could be overcome by combining NTP technology with the catalysis process, which has been successfully employed in tar reforming using various types of NTP [28,30,41]. Among the various types of NTP, dielectric barrier discharge (DBD) plasma has been most commonly used in the plasma-catalytic process because it allows for effective catalyst packing into the discharge area [42]. However, while most studies [28–34,43] have focused on plasma reforming of model tar compounds (e.g., benzene, toluene, naphthalene) derived from biomass gasification, few efforts [44–46] have been made to integrate biomass thermochemical conversion with plasma reforming for the production of hydrogen or syngas. Because cellulose accounts for about 50% of dry biomass by weight [47], understanding biomass pyrolysis and plasma-assisted reforming of cellulose is critical in developing efficient technologies for biomass conversion using plasma-based technologies.

Herein, we developed a hybrid two-stage reaction system that uses biomass pyrolysis followed by plasma-catalytic reforming to produce hydrogen. The effects of discharge power, steam, and reforming temperature on the gaseous products were investigated. Furthermore, a γ-Al_2O_3 supported Ni-Co catalyst was used in the plasma-catalytic reforming process, and the reaction performances at various operating conditions in terms of hydrogen production were evaluated.

2. Experimental

2.1. Catalyst preparation

The catalyst was prepared using the incipient wetness impregnation method, with a total metal loading weight ratio of 15 wt%. The metal precursors were cobalt nitrate hexahydrate (Aladdin, 99.5%) and nickel nitrate hexahydrate (Aladdin, 99.8%). First, a 3:1 Ni-Co ratio of cobalt nitrate hexahydrate and nickel nitrate hexahydrate was dissolved in deionized water with. The γ-Al_2O_3 support (Aladdin, 40–60 mesh) was then added to the nitrate salt solution. The resulting slurry was continuously stirred for 2 h before being aged at room temperature. It was then dried at 110 °C for 6 h before being calcined at 600 °C for 3 h at a heating rate of 5 °C. Prior to use, the catalyst was reduced for 3 h at 600 °C by H_2/Ar mixed gas (100 mL/min; 15 vol% H_2).

2.2. Experimental setup and procedures

Tandem cellulose pyrolysis and plasma-assisted reforming were carried out in a fixed bed, two-stage reaction system, as shown in Fig. 1. The first stage of cellulose pyrolysis was carried out in the first tube furnace, while the second stage of plasma reforming was carried out in the second furnace. To integrate the pyrolysis and plasma reforming processes, a 600 mm long quartz tube (24.7 mm O.D. × 16.7 mm I.D.) was used. Dry cellulose powder (0.5 g) was placed inside a quartz crucible and held in the upper of the quartz tube in the first furnace during the pyrolysis stage. A cylindrical DBD configuration was used in the plasma reforming process, with the quartz tube serving as the dielectric barrier. Specifically, a ground electrode was created by wrapping an 80 mm-long stainless-steel mesh around the quartz tube. A stainless-steel rod (300 mm Length × 14.7 mm O.D.) was used as a high voltage electrode along the axis of the quartz tube, resulting in a 1 mm discharge gap inside the quartz tube. To generate plasma in the discharge gap, an AC sinusoidal high voltage power supply (CORONA Lab CTP-2000 K) with a peak-to-peak voltage of 30 kV and a frequency of 10 kHz was used. In the second furnace, a catalyst (1 g, 40–60 mesh, if used) was placed in a portion of the discharge gap (plasma zone). The length of the discharge area was 80 mm, while the length of the catalyst bed was 10 mm. A high voltage probe (Tektronix P6015A) was used to measure the applied voltage. The voltage across an external capacitor (0.47 μF) was measured by a voltage probe (Tektronix TPP0101) to determine the amount of charge accumulated in the DBD, and a current monitor (Pearson 2877) was used to measure the current. The electrical signals were recorded by a four-channel digital oscilloscope (Tektronix MDO 3054, 500 MHz, 2.5 GS/s). The discharge power of the plasma system was determined using a standard Q-U Lissajous figure method, where Q is the charge on the external capacitor and U is the applied voltage [15]. The two-stage reaction system was continuously purged with nitrogen at a gas flow rate of 100 mL/min.

The temperature of each process was monitored by a thermocouple. A thermocouple was placed inside the quartz tube for the pyrolysis process, while another thermocouple was placed on the external surface of the quartz tube for the plasma-assisted reforming process to avoid direct contact of the thermocouple with the high voltage electrode.

The experiment began with pre-heating the second furnace to a predetermined temperature, followed by the ignition of the plasma. The first furnace was then heated to 550 °C at a heating rate of 30 °C/min to begin the pyrolysis process. When the temperature of the quartz crucible reached 150 °C in the first furnace, steam (if needed) was introduced into the second reforming stage by a syringe pump at a flow rate of 5 mL/h. Products (including tars) produced during the pyrolysis process were subsequently reformed in the plasma zone in the second stage. An ice-water cooling liquid trap condensed the liquid products in the effluent. The non-condensed gaseous products were measured using both offline and online methods. For precise offline measurement, the gases were collected after the effluent passed through an allochroic silica gel dryer. The gaseous products in the sampling bag were then analyzed by gas chromatography (Tianmei GC7900, China) equipped with a flame ionization detector and a thermal conductivity detector. Moreover, the gas products were analyzed online using an infrared syngas analyzer (ETG Ltd., Italy) to determine the time evolution of the gas composition during the reaction. In this case, the effluent gases from the dryer were introduced directly to the online gas analyzer without the use of a gas bag.

The yield of the gaseous products was calculated by the following equation.

$$Y_{product}\left(mmol/g_{cellulose}\right) = \frac{\text{moles of product (mmol)}}{\text{mass of cellulose (g)}} \quad (1)$$

The selectivity of the gaseous products was given by:

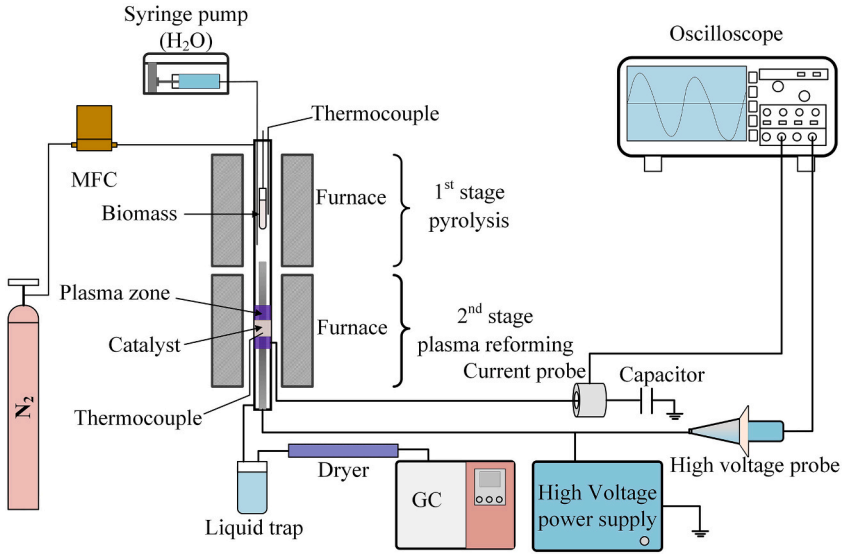

Fig. 1. Schematic diagram of the experimental setup.

$$S_{product}(\%) = \frac{\text{moles of product (mmol)}}{\text{moles of all gaseous products (mmol)}} \times 100 \quad (2)$$

3. Results and discussion

We first performed the tandem biomass pyrolysis and plasma reforming process without the use of steam and a catalyst at a pyrolysis temperature of 550 °C (1st stage) and a reforming temperature of 250 °C (2nd stage). All gaseous products increased in yield as the power increased, and the increasing trend was more noticeable for CO and H_2, with CO increasing from 1.1 mmol/g to 3.7 mmol/g and H_2 increasing from 0.2 mmol/g to 1.7 mmol/g as the discharge power increased from 0 to 15 W (Fig. 2(a)). In comparison to the heating-only reforming process (0 W in Fig. 2), using plasma in the reforming process significantly increased CO and H_2 yields by a factor of >3 and 8, respectively. Other gaseous products such as CH_4, CO_2, and C_2 - C_3 increased only

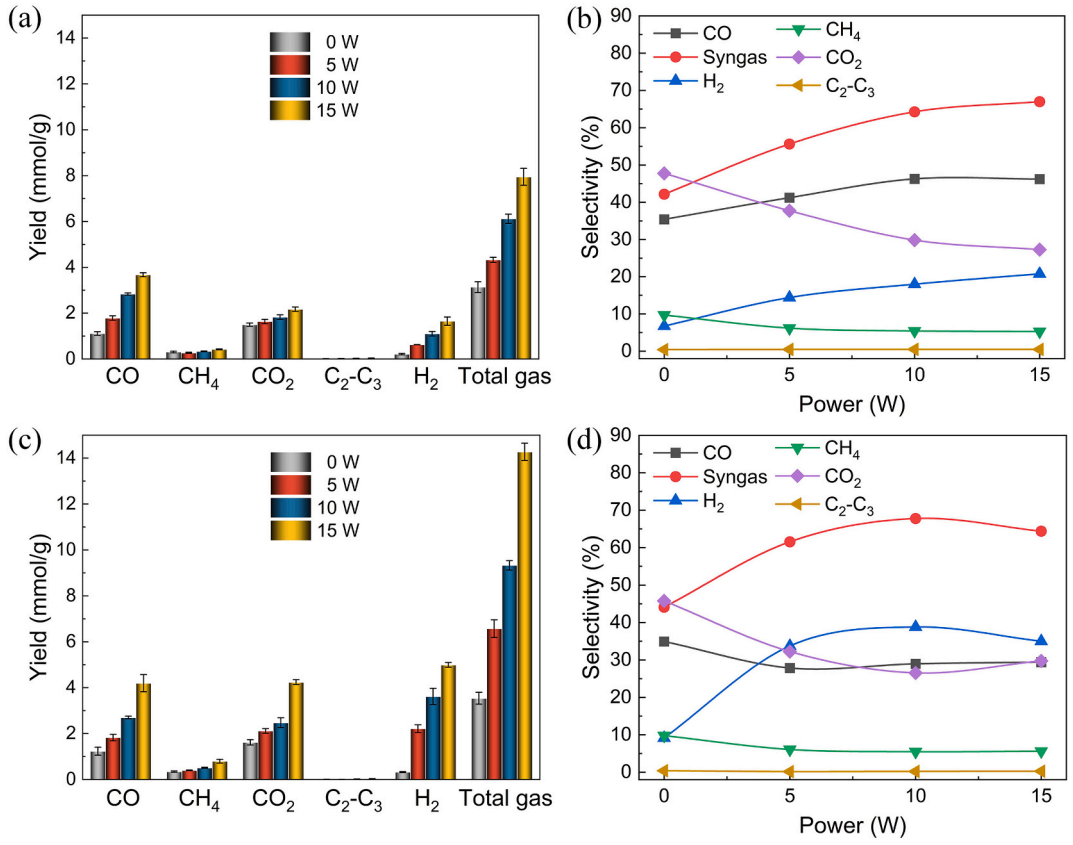

Fig. 2. Effect of discharge power on (a) the yields of gaseous products without steam, (b) the selectivity of gaseous products without steam, (c) the yields of gaseous products with steam, and (d) the selectivity of gaseous products with steam (Operating conditions: reforming temperature 250 °C; steam flow rate 5 mL/h if used; no catalyst).

slightly after the plasma was turned on. As shown in Fig. 2(b), the syngas selectivity increased significantly from 42% (0 W) to 67% (15 W). The selectivity of H_2 increased with increasing power, whereas the selectivity of CH_2 and C_2 - C_3 remained nearly constant when the discharge power was varied. However, even at the highest discharge power, the maximum H_2 yield was much lower than that obtained in the conventional thermochemical process (e.g., 18.7 mmol /g at 800 °C with a Ni-based catalyst) [23]. The previous research [29] suggested that introducing steam into the plasma reforming process can increase H_2 production via the water gas shift reaction (R1).

$$CO + H_2O \rightarrow CO_2 + H_2 \quad (R1)$$

Figs. 2(c) and 2(d) show the effects of discharge power on the yield and selectivity of gaseous products in the presence of steam at a reforming temperature of 250 °C. Similar to the results obtained without steam, the yields of all gaseous products increased with increasing discharge power. Notably, when compared to the reaction without steam, adding steam to the system significantly increased the H_2 yield and selectivity when the plasma was turned on. For example, after introducing steam into the reforming process at a discharge power of 5 W, the yield and selectivity of H_2 increased from 0.6 mmol/g to 2.2 mmol/g and from 14.4% to 33.7%, respectively. When steam was introduced into the reforming process, it increased the yields of other gaseous products as well as the total gas yield. The presence of steam in the plasma process can generate H and OH radicals through water dissociation by plasma-generated electrons (R2) and excited nitrogen species N_2* such as N_2(A) (R4). The recombination of H radicals can produce H_2 (R5), while the OH radicals could oxidize tars from the first stage pyrolysis process, yielding more gaseous products [29,48].

$$H_2O + e \rightarrow H + OH + e \quad (R2)$$

$$N_2 + e \rightarrow N_2^* + e \quad (R3)$$

$$N_2^* + H_2O \rightarrow N_2 + OH + H \quad (R4)$$

$$H + H \rightarrow H_2 \quad (R5)$$

The highest H_2 yield (5.0 mmol/g) was obtained in the plasma-assisted steam reforming at the highest discharge power, as shown in Fig. 2(c), whereas the H_2 yield dropped to only 0.3 mmol/g without plasma. On the other hand, a high power did not favor a high H_2 selectivity. For example, at a discharge power of 10 W, the H_2 selectivity reached a maximum of 39% and slightly decreased when the discharge power was increased to 15 W (Fig. 2(d)). Despite this, as shown in Fig. 2 (d), higher discharge power was beneficial to achieving a higher H_2 yield and total gas yield. Therefore, we set the discharge power to 15 W in the subsequent experiments.

Previous research has shown that the reforming temperature is critical in both conventional biomass catalytic reforming and plasma reforming processes [25,34]. To optimize the H_2 yield, we investigated the effect of reforming temperature on gaseous products. As shown in Fig. 3(a), the highest yields of CO, CH_4, C_2 - C_3, and total gas were attained at the highest reforming temperature of 550 °C, while the highest H_2 yield was obtained at 250 °C. Furthermore, increasing the reforming temperature slightly increased the CO selectivity, while H_2 selectivity decreased initially with increasing temperature and then increased slightly when further increasing the temperature from 450 °C to 550 °C (Fig. 3(b)). The highest H_2 selectivity of 35% was obtained at the lowest reforming temperature of 250 °C, and this value was cut in half when the reforming temperature was raised to 450 °C. As H_2 can be produced by both the thermal and plasma processes in the plasma-assisted reforming process with extra heating, the results suggest that

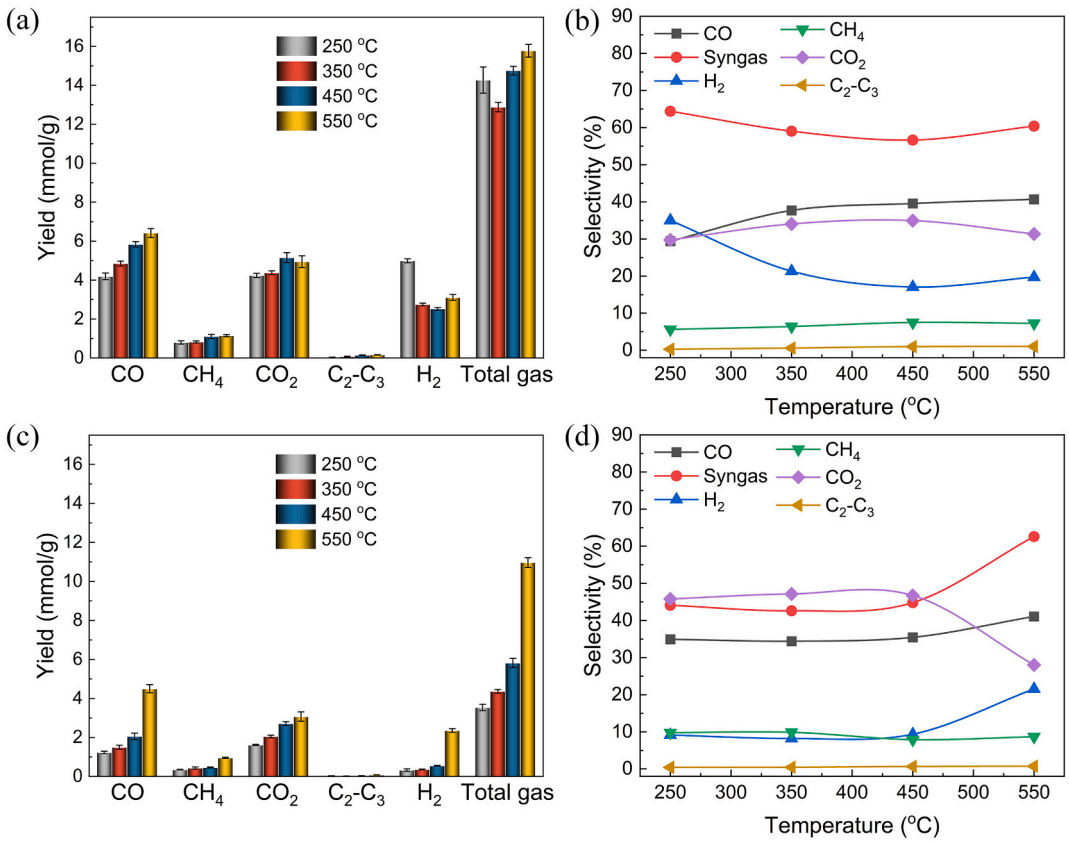

Fig. 3. Effect of reforming temperature on (a) the yields of gaseous products with plasma at a discharge power of 15 W, (b) the selectivity of gaseous products and total gas yield with plasma at a discharge power of 15 W, (c) the yield of gaseous products without plasma, and (d) the selectivity of gaseous products without plasma (Operating conditions: steam flow rate 5 mL/h; no catalyst).

increasing the reforming temperature may have a different effect on these two processes, resulting in different hydrogen production.

We performed the biomass pyrolysis and reforming process without turning on the plasma to further investigate the influence of reforming temperature on the plasma-assisted reforming process. This allowed us to understand the heating effect and how the gas yield varied with increasing reforming temperature in the absence of the plasma. As shown in Fig. 4(c), the yield of all gaseous products increased as the reforming temperature increased without plasma. Raising the temperature from 450 °C to 550 °C doubled the yields of CO, CH_4, and C_2 - C_3 and enhanced H_2 yield by a factor of four. These findings demonstrate that high temperatures were advantageous for obtaining high yields of gaseous products and high selectivity of H_2 in the absence of plasma. When the plasma was turned on, the H_2 yield was reduced by 37.7% when increasing the reforming temperature from 250 °C to 550 °C, as shown in Fig. 4(a). This finding indicates that H_2 production from cellulose reforming could be improved by either increasing the reforming temperature solely through the thermal process or by introducing plasma into the reforming process at low temperatures.

To better understand the plasma-assisted reforming process, we measured the compositions of gaseous products over time using an online infrared syngas analyzer. Fig. 4 shows the time-resolved volume proportions of gaseous products at different operating conditions. When the reforming was carried out at 250 °C without plasma (Fig. 4(a)), CO was detected firstly at around 12.5 min after starting the pyrolysis process. CO_2 and CH_4 were then produced at around 15 min, while H_2 was generated much later at around 22 min when the temperature of the pyrolysis process reached around 500 °C. In contrast, when the reforming was performed at 550 °C without plasma (Fig. 4(b)), CO, CH_4, CO_2, and H_2 were produced almost simultaneously at around 12.5 min after starting the pyrolysis process, indicating that H_2 was produced from products generated in the first stage of pyrolysis. The same

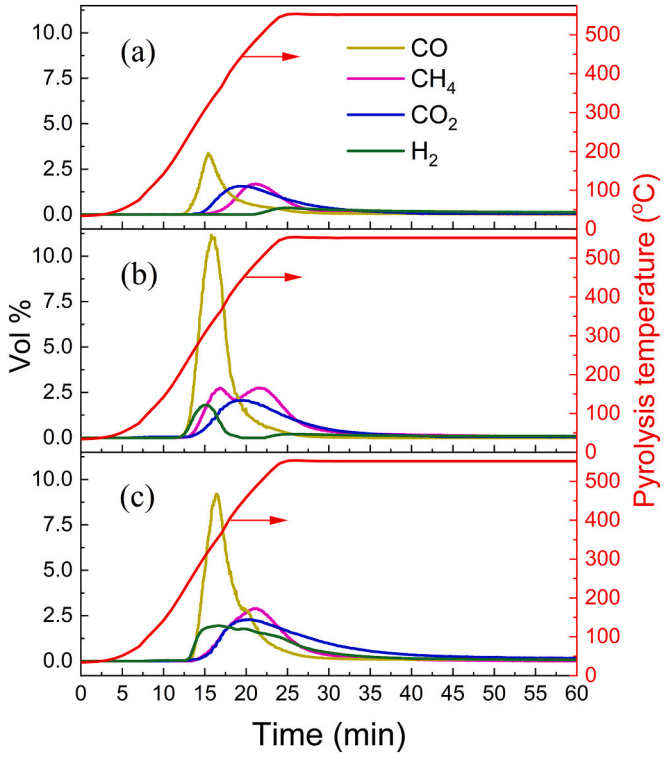

Fig. 4. Compositions of gaseous products over time under different conditions. (a) 250 °C reforming temperature without plasma, (b) 550 °C reforming temperature without plasma, and (c) 250 °C reforming temperature with plasma at a discharge power of 15 W (Operating conditions: steam flow rate 5 mL/h; no catalyst).

phenomenon was observed in plasma-assisted reforming at 250 °C, as shown in Fig. 4(c). When the reforming was performed at 550 °C without plasma, the volume of H_2 in the effluent peaked at around 15 min and then quickly dropped to around 0% at 17.5 min. Differently, in the plasma-assisted reforming at 250 °C (Fig. 3(c)), the volume proportion of H_2 peaked at around 15 min but then gradually decreased to about 0% at around 30 min, indicating that H_2 can be generated from a wider range of pyrolysis products in the plasma-assisted reforming process, generating more H_2 than heating alone at 550 °C. This finding is consistent with the off-line GC measurements (Fig. 3). Another notable difference was that two peaks in the volume proportion of CH_4 were detected when the reforming was operated with heating alone at 550 °C, as opposed to one peak detected in the plasma-assisted reforming at 250 °C. This distinction highlights the differences between high-temperature reforming and plasma-assisted reforming.

The plasma contribution to the yields of gaseous products was then investigated at different reforming temperatures. The plasma contribution was calculated by subtracting the yields of gaseous products obtained through heating alone (data in Fig. 3(c)) from the yields attained through both heating and plasma (Fig. 3(a)). The effect of heating on the reaction was thus eliminated. Fig. 5(a) shows that the plasma contribution decreased at higher reforming temperatures, and this trend was most noticeable for the H_2 yield. The percentages of plasma contribution and heating contribution during the plasma-assisted reforming process are shown in Fig. 5(b). Increasing the reforming temperature considerably reduced the percentage of plasma contribution to total gas yield. As shown in Fig. 5(c), the percentage of plasma contribution to the H_2 yield dropped significantly from 94% to 24% as the temperature increased from 250 °C to 550 °C. This finding implies that the total gas yield and H_2 yield at the highest reforming temperature are primarily attributed to the thermal effect rather than the plasma-induced promoting effect. In the plasma-assisted reforming process with extra heating, H_2 could be produced by both the thermal and plasma processes. On the one hand, increasing the temperature favored H_2 production from the thermal process, as illustrated in Fig. 3(c), where a higher temperature resulted in a higher H_2 yield. High temperatures, on the other hand, have a negative effect on H_2 production in the plasma process. As a consequence, due to a combination of the opposite effects (negative and positive), the H_2 yield in the plasma-assisted reforming process displayed irregular changes instead of simply decreasing or increasing, when increasing the reforming temperature, as shown in Fig. 3(a). In this study, the optimum reforming temperature of 250 °C, rather than higher temperatures, was identified for H_2 production in the tandem cellulose pyrolysis and non-catalytic plasma reforming process. We then set out to investigate why higher temperatures would be detrimental to the plasma process.

Liu et al. [34] found that increasing the temperature had a similar negative effect on plasma dry reforming of a model tar compound (toluene) for syngas production. Maximum toluene conversion and maximum yields of H_2, CO, and CO_2 were attained at 300 °C rather than higher temperatures of 400–500 °C in their study. They claimed that this phenomenon was caused primarily by changes in plasma characteristics due to the local thermal runaway of the quartz tube when the temperature was raised to 400–500 °C. As a result of the changes in plasma characteristics, fewer N_2 and H_2O molecules were dissociated to free radicals to react with pyrolysis products to produce gaseous products. Saleem et al. [49] reported a higher conversion of toluene at a lower reforming temperature in a DBD plasma reactor using CO_2 as a carrier gas, and they proposed that the lower conversion at higher temperatures could be attributed to faster re-association of O and CO radicals rather than O radicals reacting with toluene at higher temperatures.

In this study, we found that the reforming temperature had a direct influence on plasma characteristics. The peak-to-peak voltage across the electrodes decreased with increasing reforming temperature at a constant discharge power, as shown in Fig. 6(a). At a temperature of 250 °C, the peak-to-peak voltage across the electrodes was 14.5 kV, more than

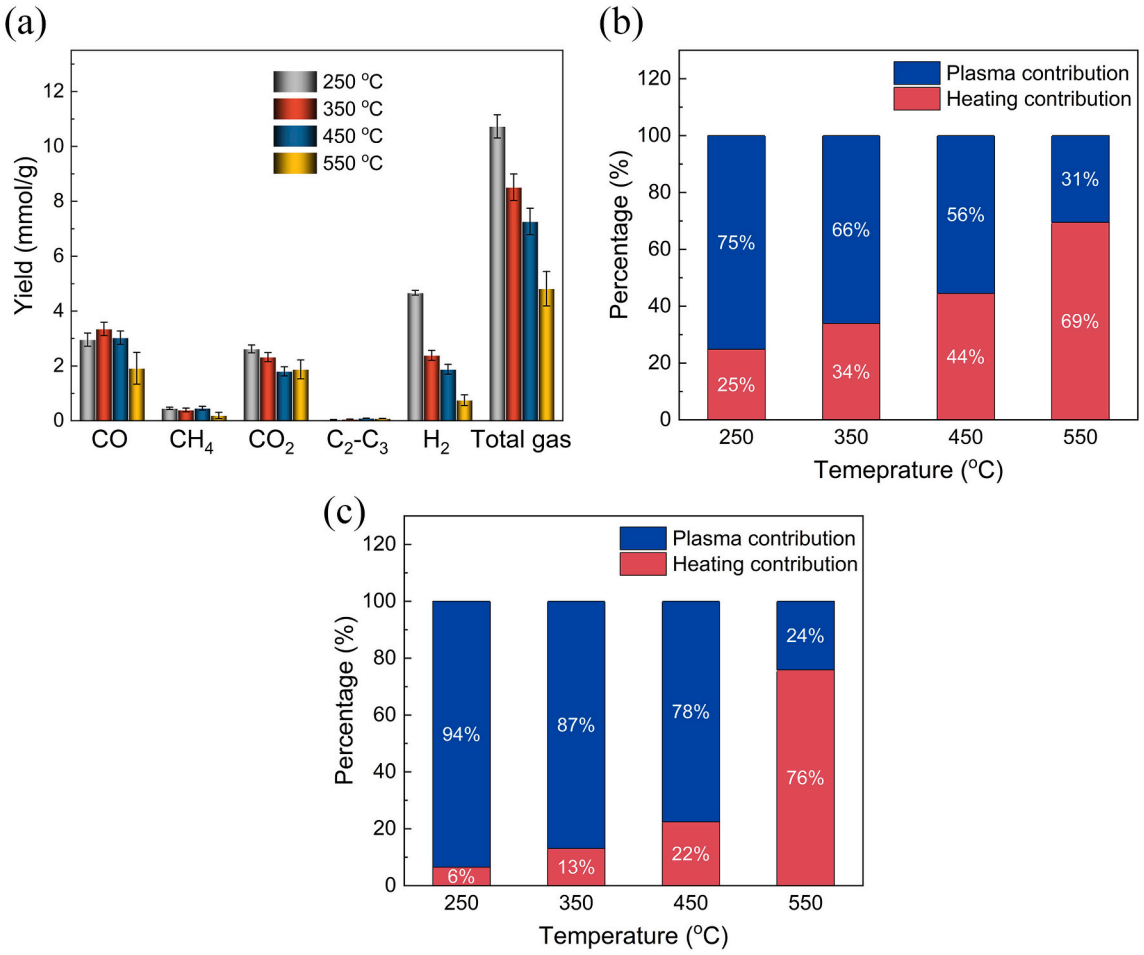

Fig. 5. Effect of reforming temperature on (a) plasma contribution to gaseous product yield, (b) plasma contribution and heating contribution to total gas yield, and (c) plasma contribution and heating contribution to H_2 yield. The plasma contribution was calculated by subtracting the data obtained by heating alone from the data obtained by heating and plasma; the heating contribution was obtained directly from the heating alone process in Fig. 3(c); the percentage of plasma or heating contribution was calculated by dividing the plasma contribution or heating contribution by the sum of the two (heating contribution + plasma contribution).

double the voltage (7.1 kV) at 550 °C reforming temperature. The lower breakdown voltage at a higher temperatures could explain the reduced voltage across the electrodes at higher temperatures, which has been experimentally confirmed by previous studies [50] and can be calculated using Paschen's law. As a result, at high temperatures, a lower voltage was required to achieve the same power. The voltage across the electrodes has a direct influence on the electric fields, which can be calculated using the Lissajous curves shown in Fig. 6(b). The detailed method for calculating the mean electric field (E) and mean reduced electric field (E/N) can be found in the literature [51,52]. Higher temperatures resulted in lower mean electric fields and lower mean reduced electric fields across the discharge gap, as displayed in Fig. 6(c). Thus, as the reforming temperatures increased, the mean electron energy decreased and these low-energetic electrons were less likely to break the molecule bonds of the tars produced by the pyrolysis, resulting in fewer gaseous products.

These findings suggest that a lower reforming temperature was preferred in the two-stage cellulose pyrolysis and plasma reforming process without a catalyst. To further improve the performance of the two-stage reaction system, we used a Ni-Co/γ-Al_2O_3 catalyst in the second-stage plasma reforming process. Previous studies found that bimetallic Ni-Co catalysts outperformed monometallic Ni and Co catalysts in terms of both catalytic activity and coke resistance in either conventional thermochemical biomass reforming or plasma-catalytic biomass reforming [30,53]. In this study, we chose a Ni-Co/γ-Al_2O_3 bimetallic catalyst with a Ni-Co ratio of 3:1.

Fig. 7(a) shows the XRD pattern of the Ni-Co/γ-Al_2O_3 catalyst. The Ni metal phase has diffraction peaks at $2\theta = 44.6°$, 51.8° and 76.5°, while the diffraction peaks of Co can be found at $2\theta = 44.2°$,51.4°and 75.7° [54]. The diffraction peaks at 38.5°and 67.1° are assigned to γ-Al_2O_3. The SEM image and elemental distribution mapping show that sufficient porosity was present, and Co and Ni species were uniformly distributed on the surface of the support (Fig. 7b).

Fig. 8 shows that packing the catalyst into the discharge area improved the total gas yield and H_2 yield regardless of the presence of plasma. Indeed, without plasma, packing the catalyst into the discharge gap enhanced the total gas yield by 117% compared to heating alone at a temperature of 250 °C, whereas adding the catalyst only increased H_2 yield by 38%. In the presence of plasma, the H_2 yield increased from 5.0 mmol/g to 7.9 mmol/g after the catalyst was packed. It is worth noting that the H_2 yield obtained in the plasma-catalytic process was greater than the sum of the plasma process and catalytic processes, indicating a synergy effect between plasma and catalyst. The plasma contributions were primarily responsible for the plasma-catalytic synergy, as shown in Fig. 8(a). The selectivity of the gaseous products under different conditions is displayed in Fig. 8(b), where the selectivity of all gaseous products in the catalytic system was nearly identical to that in the non-catalytic system regardless of the presence of plasma. The selectivity of H_2 (~35%) in plasma-assisted reforming was much higher than that achieved without plasma.

Although the above results (Fig. 3) suggest that high temperatures are not preferred for plasma reforming without a catalyst, this may not

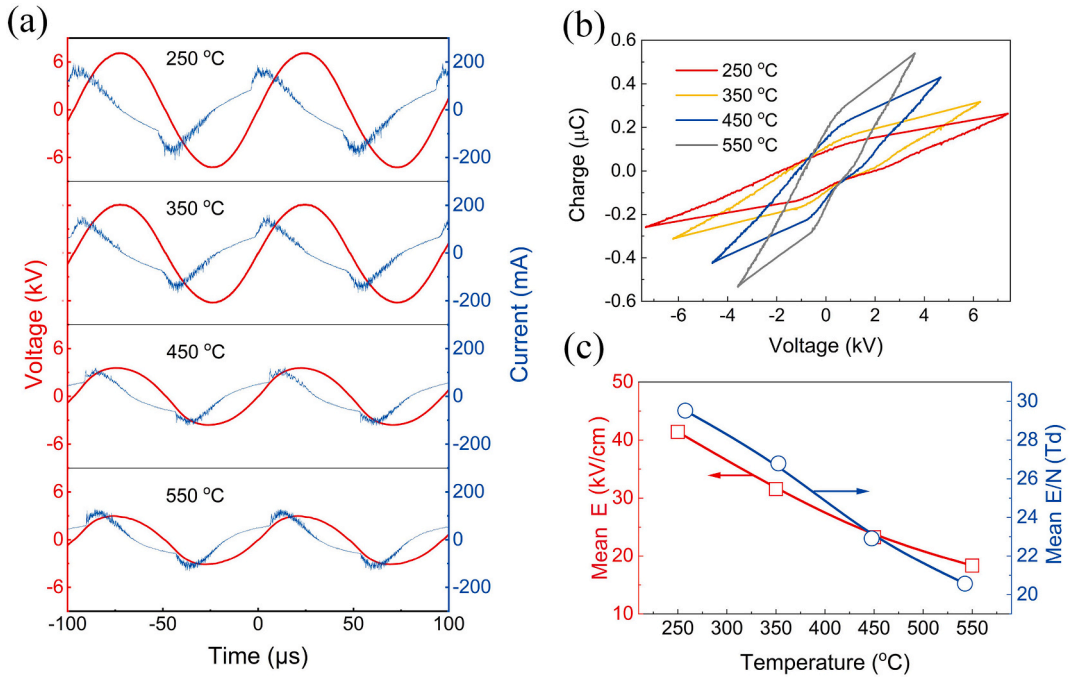

Fig. 6. Effect of reforming temperature on plasma properties at a constant discharge power (a) Voltage-current signals, (b): Lissajous curves, and (c) Mean electric fields (E) and mean reduced electric fields (E/N) at different reforming temperatures (Operating conditions: discharge power15 W, steam flow rate 5 mL/h; no catalyst).

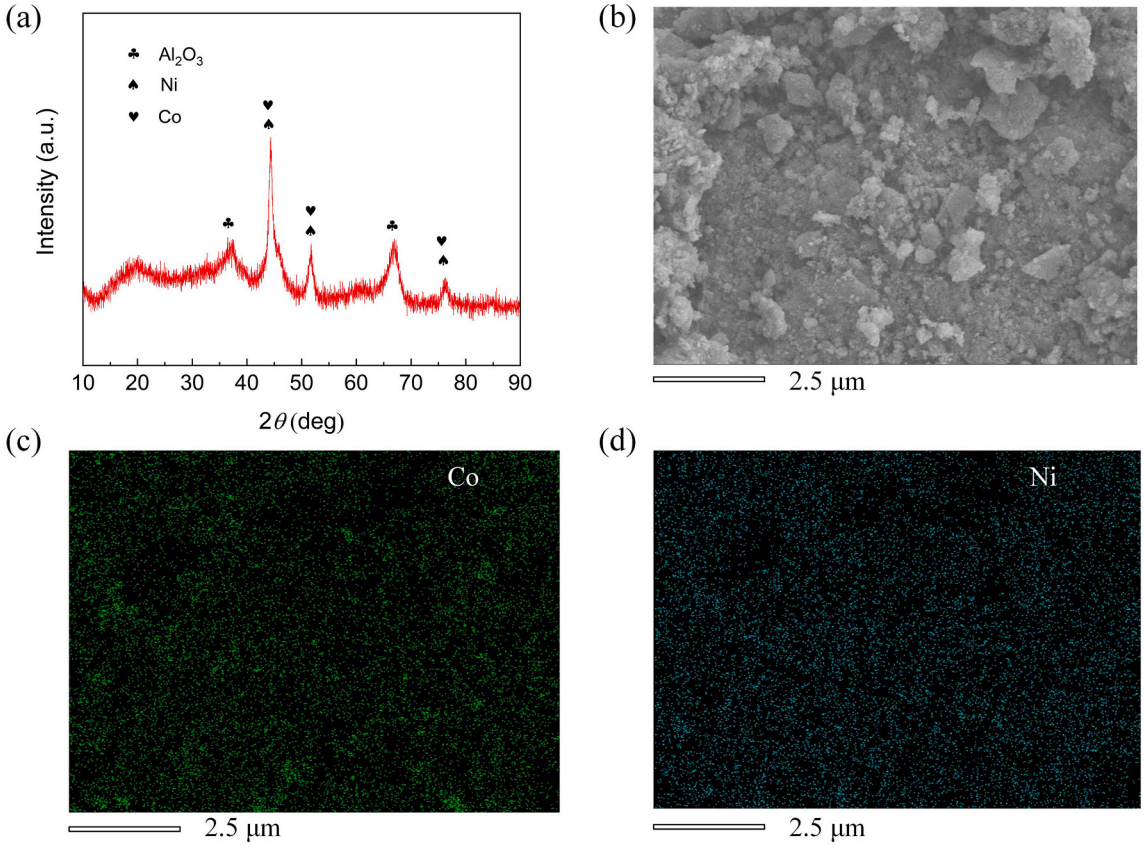

Fig. 7. (a) XRD pattern of the Ni-Co catalyst, (b) SEM image of the Ni-Co catalyst and corresponding elemental maps of (c) Co and (d) Ni.

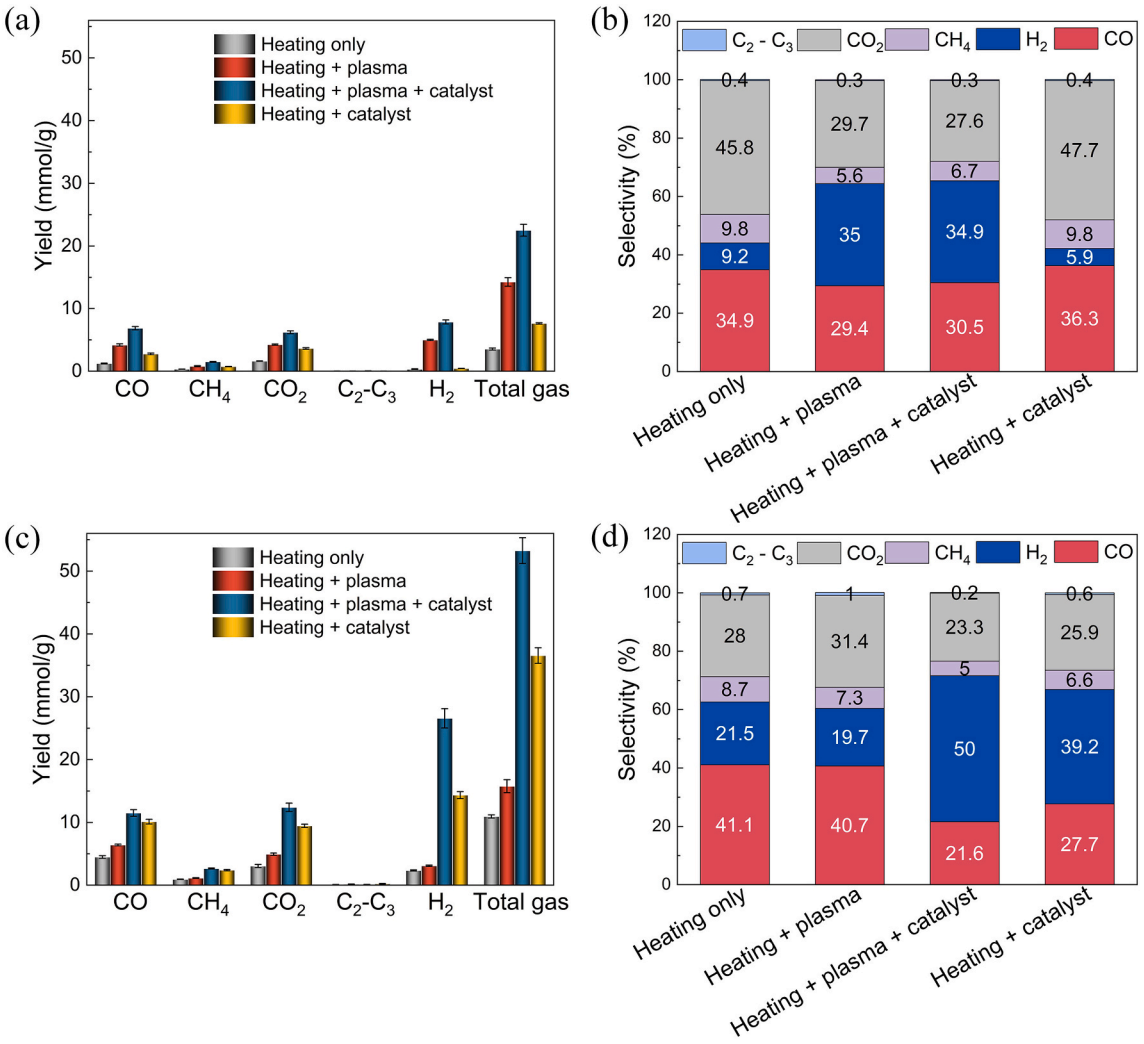

Fig. 8. Effect of catalyst on plasma-assisted reforming at different reforming temperatures: (a) (b) 250 °C and (c) (d) 550 °C (Operating conditions: catalyst 3:1 Ni-Co; steam flow rate 5 mL/h).

be the case for the plasma-catalytic process because high temperatures are always required in the conventional two-stage pyrolysis/catalytic reforming process. To improve the performance and investigate the effect of reforming temperature on the plasma-catalytic process, a series of experiments were carried out using the Ni-Co catalyst at a reforming temperature of 550 °C.

Fig. 8(c) presents that the catalyst, rather than plasma played a dominant role in the plasma-catalytic process at a reforming temperature of 550 °C, as opposed to 250 °C. At 550 °C, introducing plasma into the non-catalytic steam reforming process only moderately improved the H_2 yield and the total gas yields by 32% and 44%, respectively, compared to 324% and 1441% at 250 °C. Surprisingly, packing the catalyst into the reforming part improved performance significantly. After packing the catalyst at a reforming temperature of 550 °C, the H_2 yield and the total gas yield increased by a factor of 6 and 3, respectively. In the presence of plasma, the H_2 yield increased significantly to 26.6 mmol/g, the highest H_2 yield in this study, and 8.6 times higher than that achieved using plasma alone. The plasma-catalytic reforming process achieved the highest H_2 selectivity (50%) at a temperature of 550 °C, which was more than 10% higher than the catalytic reforming process. At 550 °C, the presence of the catalyst notably increased the H_2 selectivity, which was quite different from that at a reforming temperature of 250 °C. Similarly, a synergy effect was also observed in the plasma-catalytic reforming process at a reforming temperature of 550 °C. High temperature favored H_2 production and H_2 selectivity in the plasma-catalytic reforming process. The H_2 yield at 550 °C was comparable to that obtained using conventional thermochemical processes [23], where the reforming temperature was significantly higher (800 °C). This primary goal of this research was to optimize the operating conditions in the plasma-assisted reforming process. We believe that designing more active reforming catalysts will improve H_2 yield in the tandem biomass pyrolysis and plasma-catalytic reforming process.

4. Conclusion

In summary, we developed a tandem bioenergy process that combines cellulose pyrolysis and plasma reforming for H_2 production. The influence of the Ni-Co/Al_2O_3 catalyst on the reaction performance in the second-stage plasma reforming process was also investigated. In the non-catalytic plasma system, the addition of steam to the reforming process significantly increased the H_2 yield and selectivity of H_2. Low temperatures were preferred to enhance plasma contributions to the reforming process due to the formation of a higher reduced electric field and thus increased electron energies at lower temperatures. Online analysis of the gaseous products reveals a clear distinction between plasma contribution and temperature effect on the plasma reforming process. Compared to the non-catalytic plasma reforming process, packing Ni-Co/Al_2O_3 into the discharge gap increased the H_2 yield by

approximately 50% at a reforming temperature of 250 °C and the reforming process was dominated by the plasma. In contrast, the catalyst dominated the plasma-catalytic reforming process at a reforming temperature of 550 °C. At this temperature, the highest H_2 yield of 26.6 mmol/g was obtained using the Ni-Co/Al_2O_3 catalyst, which was more than 8 times and about 100% higher than that obtained using plasma alone and catalyst alone. This study demonstrates that a high H_2 yield can be achieved using a plasma-catalytic process at a low reforming temperature, indicating that plasma technology has a promising future in biomass conversion.

Data access statement

The data supporting the findings of this study are available upon reasonable request from the corresponding authors.

CRediT authorship contribution statement

Weitao Wang: Conceptualization, Methodology, Investigation, Formal analysis, Visualization, Writing – original draft, Writing – review & editing. **Yan Ma:** Investigation. **Guoxing Chen:** Formal analysis, Writing – review & editing. **Cui Quan:** Supervision, Writing – review & editing. **Jale Yanik:** Formal analysis, Writing – review & editing, Funding acquisition. **Ningbo Gao:** Conceptualization, Supervision, Resources, Writing – review & editing, Project administration, Funding acquisition. **Xin Tu:** Conceptualization, Supervision, Resources, Writing – review & editing, Project administration, Funding acquisition.

Declaration of Competing Interest

The authors declare that they have no known competing financial interests or personal relationships that could have appeared to influence the work reported in this paper.

Acknowledgements

This project has received the funding from the European Union's Horizon 2020 Research and Innovation Programme under the Marie Sklodowska-Curie Grant Agreement (No. 823745). C. Quan and N. Gao gratefully acknowledge funding from the Science and Technology Exchange Project of the Chinese Ministry of Science and Technology (No. 2021-12-2) and the Education Cooperation Project between China and Central Eastern European Countries (No. 2021086). X. Tu gratefully acknowledges the British Council Newton Fund Institutional Links Grant (No. 623389161). J. Yanik gratefully acknowledges funding from the Scientific and Technological Research Council of Turkey (TUBITAK Project Contract no. 219M123). W. Wang thanks the University of Liverpool and the Chinese Scholarship Council for funding this PhD.

References

[1] P. Sharma, B. Gupta, M. Pandey, K.S. Bisen, P. Baredar, Downdraft biomass gasification: a review on concepts, designs analysis, modelling and recent advances, Mater. Today: Proceed. 46 (2021) 5333–5341.
[2] E. Barbuzza, G. Buceti, A. Pozio, M. Santarelli, S. Tosti, Gasification of wood biomass with renewable hydrogen for the production of synthetic natural gas, Fuel 242 (2019) 520–531.
[3] J. Yu, Q. Guo, Y. Gong, L. Ding, J. Wang, G. Yu, A review of the effects of alkali and alkaline earth metal species on biomass gasification, Fuel Process. Technol. 214 (2021), 106723.
[4] D.E. Resasco, B. Wang, D. Sabatini, Distributed processes for biomass conversion could aid UN Sustainable Development Goals, Nature Catalys. 1 (2018) 731–735.
[5] F. Ueckerdt, C. Bauer, A. Dirnaichner, J. Everall, R. Sacchi, G. Luderer, Potential and risks of hydrogen-based e-fuels in climate change mitigation, Nat. Clim. Chang. 11 (2021) 384–393.
[6] L. Zhang, T.U. Rao, J. Wang, D. Ren, S. Sirisommboonchai, C. Choi, H. Machida, Z. Huo, K. Norinaga, A review of thermal catalytic and electrochemical hydrogenation approaches for converting biomass-derived compounds to high-value chemicals and fuels, Fuel Process. Technol. 226 (2022), 107097.
[7] A. Kalair, N. Abas, M.S. Saleem, A.R. Kalair, N. Khan, Role of energy storage systems in energy transition from fossil fuels to renewables, Energy Stor. 3 (2021), e135.
[8] B. Rice, D. Ainslie, A Burning Issue: Biomass is the Biggest Source of Renewable Energy Consumed in the UK. https://www.ons.gov.uk/economy/environmentalaccounts/articles/aburningissuebiomassisthebiggestsourceofrenewableenergyconsumedintheuk/2019-08-30, 2019 (accessed 30 August 2019).
[9] D. Cheng, H.H. Ngo, W. Guo, S.W. Chang, D.D. Nguyen, L. Deng, Z. Chen, Y. Ye, X. T. Bui, N.B. Hoang, Advanced strategies for enhancing dark fermentative biohydrogen production from biowaste towards sustainable environment, Bioresour. Technol. 351 (2022), 127045.
[10] M. Aziz, A. Darmawan, F.B. Juangsa, Hydrogen production from biomasses and wastes: a technological review, Int. J. Hydrog. Energy 46 (2021) 33756–33781.
[11] N. Hanchate, S. Ramani, C. Mathpati, V.H. Dalvi, Biomass gasification using dual fluidized bed gasification systems: a review, J. Clean. Prod. 280 (2021), 123148.
[12] N.A. Ali, M. Ismail, Advanced hydrogen storage of the Mg–Na–Al system: a review, J. Magnes. Alloys 9 (2021) 1111–1122.
[13] A.M. Oliveira, R.R. Beswick, Y. Yan, A green hydrogen economy for a renewable energy society, Current Opin. Chem. Eng. 33 (2021), 100701.
[14] H. Zhang, L. Wang, F. Maréchal, U. Desideri, Techno-economic comparison of green ammonia production processes, Appl. Energy 259 (2020), 114135.
[15] Y. Wang, M. Craven, X. Yu, J. Ding, P. Bryant, J. Huang, X. Tu, Plasma-enhanced catalytic synthesis of ammonia over a Ni/Al_2O_3 catalyst at near-room temperature: insights into the importance of the catalyst surface on the reaction mechanism, ACS Catal. 9 (2019) 10780–10793.
[16] I. Ro, Y. Liu, M.R. Ball, D.H. Jackson, J.P. Chada, C. Sener, T.F. Kuech, R.J. Madon, G.W. Huber, J.A. Dumesic, Role of the Cu-ZrO_2 interfacial sites for conversion of ethanol to ethyl acetate and synthesis of methanol from CO_2 and H_2, ACS Catal. 6 (2016) 7040–7050.
[17] J. Kang, S. He, W. Zhou, Z. Shen, Y. Li, M. Chen, Q. Zhang, Y. Wang, Single-pass transformation of syngas into ethanol with high selectivity by triple tandem catalysis, Nat. Commun. 11 (2020) 1–11.
[18] S. Sharma, S.K. Ghoshal, Hydrogen the future transportation fuel: from production to applications, Renew. Sust. Energ. Rev. 43 (2015) 1151–1158.
[19] Z. Xiong, Y. Xiong, Q. Li, H. Han, W. Deng, J. Xu, L. Jiang, S. Su, S. Hu, Y. Wang, Effects of vapor−/solid-phase interactions among cellulose, hemicellulose and lignin on the formation of heavy components in bio-oil during pyrolysis, Fuel Process. Technol. 225 (2022), 107042.
[20] X. Huang, J. Ren, J.-Y. Ran, C.-L. Qin, Z.-Q. Yang, J.-P. Cao, Recent advances in pyrolysis of cellulose to value-added chemicals, Fuel Process. Technol. 229 (2022), 107175.
[21] T. Jin, H. Wang, J. Peng, Y. Wu, Z. Huang, X. Tian, M. Ding, Catalytic pyrolysis of lignin with metal-modified HZSM-5 as catalysts for monocyclic aromatic hydrocarbons production, Fuel Process. Technol. 230 (2022), 107201.
[22] E. Shayan, V. Zare, I. Mirzaee, Hydrogen production from biomass gasification; a theoretical comparison of using different gasification agents, Energy Convers. Manag. 159 (2018) 30–41.
[23] C. Wu, Z. Wang, J. Huang, P.T. Williams, Pyrolysis/gasification of cellulose, hemicellulose and lignin for hydrogen production in the presence of various nickel-based catalysts, Fuel 106 (2013) 697–706.
[24] M. Ye, Y. Tao, F. Jin, H. Ling, C. Wu, P.T. Williams, J. Huang, Enhancing hydrogen production from the pyrolysis-gasification of biomass by size-confined Ni catalysts on acidic MCM-41 supports, Catal. Today 307 (2018) 154–161.
[25] Y. Chai, N. Gao, M. Wang, C. Wu, H_2 production from co-pyrolysis/gasification of waste plastics and biomass under novel catalyst Ni-CaO-C, Chem. Eng. J. 382 (2020), 122947.
[26] Z. Zhang, C. Qin, Z. Ou, H. Xia, J. Ran, C. Wu, Experimental and thermodynamic study on sorption-enhanced steam reforming of toluene for H_2 production using the mixture of Ni/perovskite-CaO, Fuel 305 (2021), 121447.
[27] D. Xu, Y. Xiong, J. Ye, Y. Su, Q. Dong, S. Zhang, Performances of syngas production and deposited coke regulation during co-gasification of biomass and plastic wastes over Ni/γ-Al_2O_3 catalyst: Role of biomass to plastic ratio in feedstock, Chem. Eng. J. 392 (2020), 123728.
[28] L. Liu, Z. Zhang, S. Das, S. Kawi, Reforming of tar from biomass gasification in a hybrid catalysis-plasma system: a review, Appl. Catal. B Environ. 250 (2019) 250–272.
[29] Y. Wang, H. Yang, X. Tu, Plasma reforming of naphthalene as a tar model compound of biomass gasification, Energy Convers. Manag. 187 (2019) 593–604.
[30] D. Mei, S. Liu, Y. Wang, H. Yang, Z. Bo, X. Tu, Enhanced reforming of mixed biomass tar model compounds using a hybrid gliding arc plasma catalytic process, Catal. Today 337 (2019) 225–233.
[31] B. Xu, J. Xie, X. Yin, H. Liu, C. Sun, C. Wu, Mechanisms of toluene removal in relation to the main components of biosyngas in a catalytic nonthermal plasma process, Energy Fuel 33 (2019) 4287–4301.
[32] R. Xu, X. Kong, H. Zhang, P.M. Ruya, X. Li, Destruction of gasification tar over Ni catalysts in a modified rotating gliding arc plasma reactor: effect of catalyst position and nickel loading, Fuel 289 (2021), 119742.
[33] R. Xu, F. Zhu, H. Zhang, P.M. Ruya, X. Kong, L. Li, X. Li, Simultaneous removal of toluene, naphthalene, and phenol as tar surrogates in a rotating gliding arc discharge reactor, Energy Fuel 34 (2020) 2045–2054.
[34] L. Liu, Q. Wang, J. Song, X. Yang, Y. Sun, Dry reforming of model biomass pyrolysis products to syngas by dielectric barrier discharge plasma, Int. J. Hydrog. Energy 43 (2018) 10281–10293.
[35] I. Aminu, M.A. Nahil, P.T. Williams, Hydrogen production by pyrolysis–nonthermal plasma/catalytic reforming of waste plastic over different catalyst support materials, Energy Fuel 36 (2022) 3788–3801.

[36] G. Chen, X. Tu, G. Homm, A. Weidenkaff, Plasma pyrolysis for a sustainable hydrogen economy, Nat. Rev. Mater. 7 (2022) 333–334.
[37] H. Zhang, X. Li, F. Zhu, K. Cen, C. Du, X. Tu, Plasma assisted dry reforming of methanol for clean syngas production and high-efficiency CO_2 conversion, Chem. Eng. J. 310 (2017) 114–119.
[38] H. Zhang, W. Wang, X. Li, L. Han, M. Yan, Y. Zhong, X. Tu, Plasma activation of methane for hydrogen production in a N_2 rotating gliding arc warm plasma: a chemical kinetics study, Chem. Eng. J. 345 (2018) 67–78.
[39] H. Conrads, M. Schmidt, Plasma generation and plasma sources, Plasma Sources Sci. Technol. 9 (2000) 441.
[40] D. Mei, P. Zhang, S. Liu, L. Ding, Y. Ma, R. Zhou, H. Gu, Z. Fang, P.J. Cullen, X. Tu, Highly efficient reforming of toluene to syngas in a gliding arc plasma reactor, J. Energy Inst. 98 (2021) 131–143.
[41] S. Liu, D. Mei, M. Nahil, S. Gadkari, S. Gu, P. Williams, X. Tu, Hybrid plasma-catalytic steam reforming of toluene as a biomass tar model compound over Ni/Al_2O_3 catalysts, Fuel Process. Technol. 166 (2017) 269–275.
[42] A. Bogaerts, X. Tu, J.C. Whitehead, G. Centi, L. Lefferts, O. Guaitella, F. Azzolina-Jury, H.-H. Kim, A.B. Murphy, W.F. Schneider, T. Nozaki, J.C. Hicks, A. Rousseau, F. Thevenet, A. Khacef, M. Carreon, The 2020 plasma catalysis roadmap, J. Phys. D. Appl. Phys. 53 (2020), 443001.
[43] H. Zhang, R. Xu, J. Ananthanarasimhan, J. Zheng, J. Wan, K. Wang, B. Lan, J. Yan, X. Li, Destruction of biomass tar model compound in a rotating gliding arc plasma catalytic system: contribution of typical transition metals in Ni-based bimetallic catalyst, Fuel 323 (2022), 124385.
[44] M. Craven, Y. Wang, H. Yang, C. Wu, X. Tu, Integrated gasification and non-thermal plasma-catalysis system for cleaner syngas production from cellulose, IOP SciNotes 1 (2020), 024001.
[45] E. Blanquet, M.A. Nahil, P.T. Williams, Enhanced hydrogen-rich gas production from waste biomass using pyrolysis with non-thermal plasma-catalysis, Catal. Today 337 (2019) 216–224.
[46] E. Blanquet, P.T. Williams, Biomass pyrolysis coupled with non-thermal plasma/catalysis for hydrogen production: Influence of biomass components and catalyst properties, J. Anal. Appl. Pyrolysis 159 (2021), 105325.
[47] J. Lédé, Cellulose pyrolysis kinetics: an historical review on the existence and role of intermediate active cellulose, J. Anal. Appl. Pyrolysis 94 (2012) 17–32.
[48] D. Mei, Y. Wang, S. Liu, M. Alliati, H. Yang, X. Tu, Plasma reforming of biomass gasification tars using mixed naphthalene and toluene as model compounds, Energy Convers. Manag. 195 (2019) 409–419.
[49] F. Saleem, K. Zhang, A. Harvey, Role of CO_2 in the conversion of toluene as a tar surrogate in a nonthermal plasma dielectric barrier discharge reactor, Energy Fuel 32 (2018) 5164–5170.
[50] H.S. Uhm, S.J. Jung, H.S. Kim, Influence of gas temperature on electrical breakdown in cylindrical electrodes, J. Korean Phys. Soc. 42 (2003) S989–S993.
[51] P.W.C. Groen, A. Wolf, T. Righart, M. Van De Sanden, F. Peeters, W. Bongers, Numerical model for the determination of the reduced electric field in a CO_2 microwave plasma derived by the principle of impedance matching, Plasma Sources Sci. Technol. 28 (2019), 075016.
[52] F. Rodrigues, J. Pascoa, M. Trancossi, Heat generation mechanisms of DBD plasma actuators, Exp. Thermal Fluid Sci. 90 (2018) 55–65.
[53] L. Wang, D. Li, M. Koike, H. Watanabe, Y. Xu, Y. Nakagawa, K. Tomishige, Catalytic performance and characterization of Ni–Co catalysts for the steam reforming of biomass tar to synthesis gas, Fuel 112 (2013) 654–661.
[54] X. Zhao, G. Lu, Modulating and controlling active species dispersion over Ni–Co bimetallic catalysts for enhancement of hydrogen production of ethanol steam reforming, Int. J. Hydrog. Energy 41 (2016) 3349–3362.